scientific reports

OPEN

Basal forebrain volume and metabolism in carriers of the Colombian mutation for autosomal dominant Alzheimer's disease

Stefan Teipel[1,2✉], Alice Grazia[1], Martin Dyrba[1], Michel J. Grothe[3] & Nunzio Pomara[4]

We aimed to study atrophy and glucose metabolism of the cholinergic basal forebrain in non-demented mutation carriers for autosomal dominant Alzheimer's disease (ADAD). We determined the level of evidence for or against atrophy and impaired metabolism of the basal forebrain in 167 non-demented carriers of the Colombian PSEN1 E280A mutation and 75 age- and sex-matched non-mutation carriers of the same kindred using a Bayesian analysis framework. We analyzed baseline MRI, amyloid PET, and FDG-PET scans of the Alzheimer's Prevention Initiative ADAD Colombia Trial. We found moderate evidence against an association of carrier status with basal forebrain volume (Bayes factor (BF_{10}) = 0.182). We found moderate evidence against a difference of basal forebrain metabolism (BF_{10} = 0.167). There was only inconclusive evidence for an association between basal forebrain volume and delayed memory and attention (BF_{10} = 0.884 and 0.184, respectively), and between basal forebrain volume and global amyloid load (BF_{10} = 2.1). Our results distinguish PSEN1 E280A mutation carriers from sporadic AD cases in which cholinergic involvement of the basal forebrain is already detectable in the preclinical and prodromal stages. This indicates an important difference between ADAD and sporadic AD in terms of pathogenesis and potential treatment targets.

Pathological evidence suggests a cholinergic deficit in dementia stages of sporadic Alzheimer's disease (AD), characterized by reduced choline-acetyl transferase and acetylcholinesterase activity in cortical target regions of cholinergic projections from the basal forebrain, particularly the Nucleus basalis Meynert (NbM), and loss of cholinergic neurons in the NbM[1]. In early stages of sporadic AD, i.e. in people with an antemortem diagnosis of mild cognitive impairment (MCI), cholinergic basal forebrain neurons exhibited neurofibrillary tangles and cell shrinkage associated with accumulation of cortical amyloid[2,3], but not yet frank neuron loss[4].

Consistently, volumetric MRI studies demonstrated atrophy of the basal forebrain in sporadic MCI cases[5–9] and amyloid positive cognitively normal people[10–12]. FDG-PET studies found increased basal forebrain metabolic rate in sporadic MCI cases compared to normal controls[13,14], which may indicate compensatory upregulation of regional metabolism in early stages of neurodegeneration or loss of cortical GABAergic inhibitory neurons. In contrast to sporadic AD, basal forebrain has not yet been studied in humans with autosomal dominant AD (ADAD).

Here, we studied baseline data from participants of the API Colombian trial recruited from a kindred harboring the Colombian NM_000021:c.839A>C, p.(Glu280Ala) (commonly known as PSEN1 E280A) mutation[15], which is associated with early onset ADAD[16]. We determined volume and metabolism of the cholinergic basal forebrain in association with mutation carrier status and levels of cerebral amyloid. We hypothesized that non-demented PSEN1 E280A mutation carriers would exhibit atrophy and increased glucose metabolism of the basal forebrain compared with non-carriers, suggesting an early cholinergic deficit and compensatory hyperactivity. For comparison, we examined hippocampal atrophy, as some[17,18], but not all[19,20] studies have shown hippocampal

[1]Deutsches Zentrum für Neurodegenerative Erkrankungen (DZNE), Gehlsheimer Str. 20, 18147 Rostock, Germany. [2]Department of Psychosomatic Medicine, University Medicine Rostock, Gehlsheimer Str. 20, 18147 Rostock, Germany. [3]CIEN Foundation/Queen Sofia Foundation Alzheimer Center, Madrid, Spain. [4]Geriatric Psychiatry Division, Nathan Kline Institute/Department of Psychiatry and Pathology, NYU Grossman School of Medicine, Orangeburg, NY, USA. ✉email: stefan.teipel@med.uni-rostock.de

atrophy in prodromal ADAD. In addition, we used thalamus as comparison region that had been found to be atrophied in different presenilin mutations[21–24]. We used a Bayesian analysis framework for two reasons. First, a Bayesian approach allowed us to directly quantify evidence for and against an effect. Thus, in case of absence of an effect, we could directly quantify how plausible the evidence was for the absence of an effect[25,26]. This is different for the frequentist null hypothesis significance testing. Here, the p value indicates the probability with which the same or an even more extreme effect will be found in hypothetical repetitions of the same experiment if the hypothesis of no effect is true[27]. Secondly, the Bayesian credible interval represents the bounds within which the true value is expected to lie with 95% probability given the observed data ([28], chapter 11.3). The frequentist confidence interval relates to long-term realizations of the parameter value in future hypothetical experiments[29]. Given this rather non-intuitive meaning, the frequentist confidence interval is often misinterpreted as if it were a Bayesian credible interval. Evidence for early cholinergic changes in autosomal dominant AD would underscore the phenotypic similarity between sporadic AD and ADAD, whereas evidence for the absence of such effects would point to important differences between ADAD and sporadic AD in terms of pathogenesis and treatment targets[30].

Results
Demographics
Overall 242 cases, including 167 mutation carriers and 75 non-mutation carrier family members, met inclusion criteria. Evidence was extremely in favor of a higher age in the non-carriers, but evidence was inconclusive or absent for a difference in sex, years of education, MMSE, and CDR scores (see Table 1 for details).

Association of carrier status with brain volumes
We found moderate evidence for no association of carrier status with normalized basal forebrain volume ($BF_{10} = 0.182$) or hippocampus volume ($BF_{10} = 0.163$), controlling for age, sex, and CDR score. When we repeated this analysis with an unidirectional prior derived from our a priori hypothesis, i.e. carriers were expected to have smaller volumes than non-carriers, the evidence for absence of an effect became even stronger with a BF_{10} of 0.104 for basal forebrain, and a BF_{10} of 0.116 for hippocampus, i.e. absence of a smaller basal forebrain or hippocampus volume in carriers than in non-carriers was 8.6 to 9.6 times more likely than presence of such an effect. We found moderate evidence for an smaller thalamus volume in mutation carriers ($BF_{10} = 8.38$), controlling for age group, sex, and CDR score. This effect was preserved with a BF_{10} of 7.8 after including ApoE epsilon 4 genotype into the null model. Details are shown in Fig. 1.

Association of carrier status and brain volumes with cognitive scores
Within the CDR 0 cases, we found extreme evidence for an association of carrier status with delayed recall performance (RBANS delayed memory) ($BF_{10} = 12,062.2$), indicating poorer performance in mutation carriers, controlling for age group, education, and sex. Evidence was inconclusive for attention ($BF_{10} = 0.454$). Details are shown in Fig. 2.

Both in CDR 0 and in all cases combined, we found evidence against an association of normalized basal forebrain and hippocampus volumes with delayed recall. Evidence was in favor of an association of thalamus volume with delayed recall (Fig. 3), both in CDR 0 and in all cases combined, but not with attention, after controlling for age, sex, education, and carrier status. Details are shown in Table 2. Numbers in the CDR 0.5 subgroup were too small to run meaningful regression analyses separately in this group.

Voxel based analysis of MRI data
We found small areas of reduced volumes in PSEN1 E280A carriers compared with non-carriers in right predominant medial thalamus, consistent with the region of interest based analyses (Fig. 4), as well as small areas of increased brain volumes in carriers vs. non-carriers in bilateral fusiform gyrus, middle temporal gyrus and cerebellum.

	PSEN1 E280A carriers	Noncarriers
N (female/male)[1]	101/66	50/25
Age group (30–34/35–39/40–44/45–49/50–54 years)[2]	71/48/30/17/1	9/18/19/20/9
CDR global (0/0.5)[3]	150/17	70/5
MMSE score (95% credible interval)[4]	28.8 (28.6–29.0)	29.2 (29.0–29.4)
Education (95% credible interval) [years][5]	8.8 (8.1–9.4)	8.5 (7.5–9.5)

Table 1. Demographic characteristics. [1]Bayesian contingency table: Bayes factor shows moderate evidence for no difference in proportion of sex between groups ($BF_{10} = 0.251$). [2]Bayesian contingency table: Bayes factor shows extreme evidence for a difference in proportion of age-groups between groups ($BF_{10} = 3.8 \times 10^6$), with higher age in the noncarriers. [3]Bayesian contingency table: Bayes factor shows moderate evidence for no difference in proportion of CDR global scores between groups ($BF_{10} = 0.138$). [4]Bayesian t-test: Bayes factor shows inconclusive evidence for a difference between groups ($BF_{10} = 1.384$). [5]Bayesian t-test: Bayes factor shows moderate evidence for no difference between groups ($BF_{10} = 0.168$).
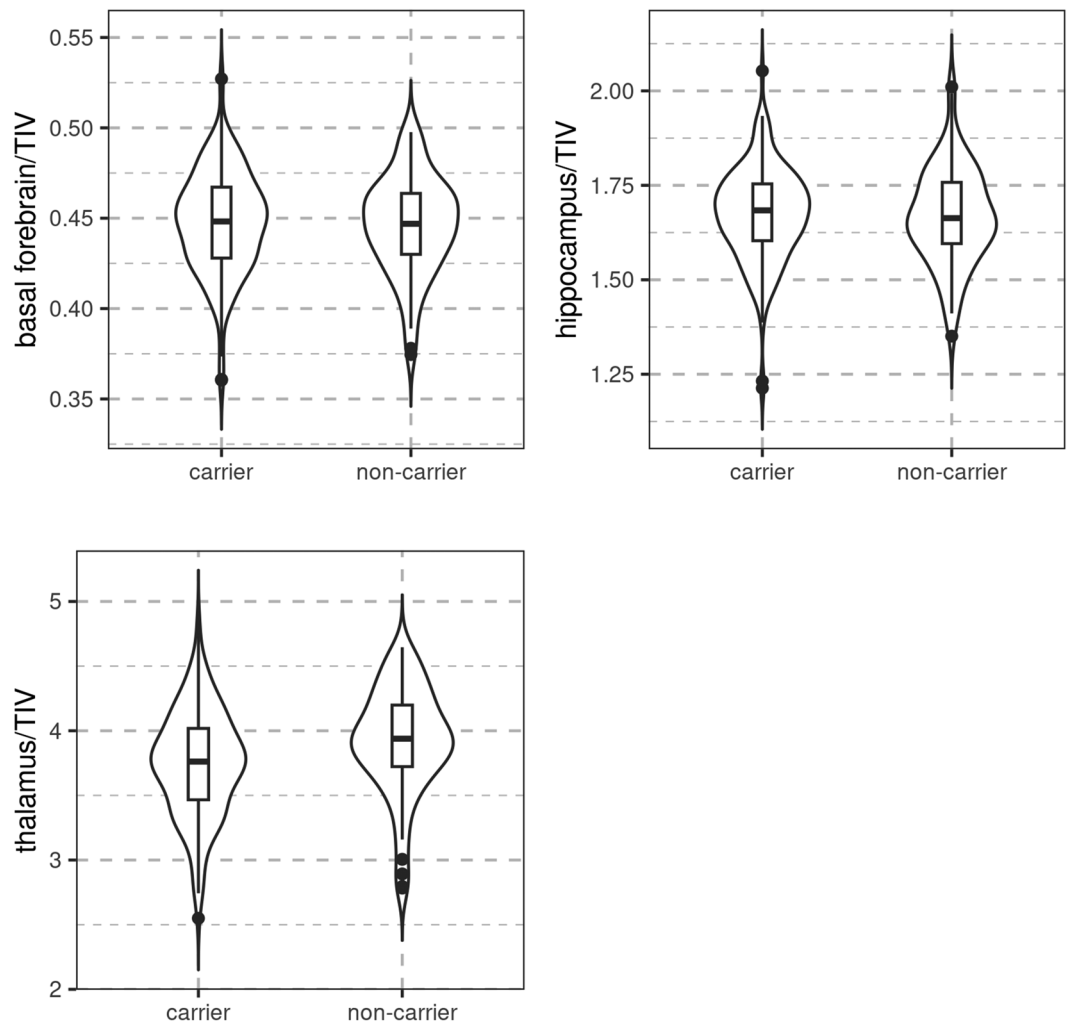
Figure 1. Association of carrier status with brain volumes. Boxplots and violin plots featuring volumes of basal forebrain, hippocampus, and thalamus according to mutation carrier status. Each volumetric measure was normalized to total intracranial volume (TIV).

Association of carrier status with regional metabolism

In an ANCOVA model, evidence was in favor of no difference between mutation carriers and non-carriers in pons normalized basal forebrain signal ($BF_{10} = 0.167$), controlling for age, sex, and CDR score, suggesting a relatively preserved basal forebrain metabolism in mutation carriers (Fig. 5). We found anecdotal evidence against a difference of hippocampus metabolism ($BF_{10} = 0.582$) and moderate evidence against a difference of thalamus metabolism ($BF_{10} = 0.165$) in mutation carriers compared with non-carriers.

Voxel based analysis of FDG-PET data

We found reduced globally-normalized metabolism in bilateral superior parietal and posterior cingulate cortex, and increased metabolism in cerebellum and basal forebrain regions in mutation carriers (Fig. 6).

Amyloid sensitive AV45-PET data across groups

K-means clustering with R command kmeans resulted in two clusters with a threshold of approximately > 1.12 for amyloid positivity (Supplementary Fig. 1). We found extreme evidence in favor of an effect of carrier status on amyloid positivity (contingency table test, $BF_{10} = 2.2 \times 10^{19}$) with 57% of the mutation carriers being amyloid positive but none of the non-mutation carriers, see Supplementary Table 1 for details.

Association of volumes with global AV45-PET signal

We found inconclusive evidence for an association of global AV45-PET signal with normalized basal forebrain ($BF_{10} = 2.1$) or hippocampus volume ($BF_{10} = 1.4$), but very strong evidence in favor of an association of global AV45-PET signal with thalamus volume ($BF_{10} = 99.0$). More amyloid signal was associated with smaller thalamus volume, after controlling for mutation carrier status. Details can be found in Supplementary Fig. 2. The effect of
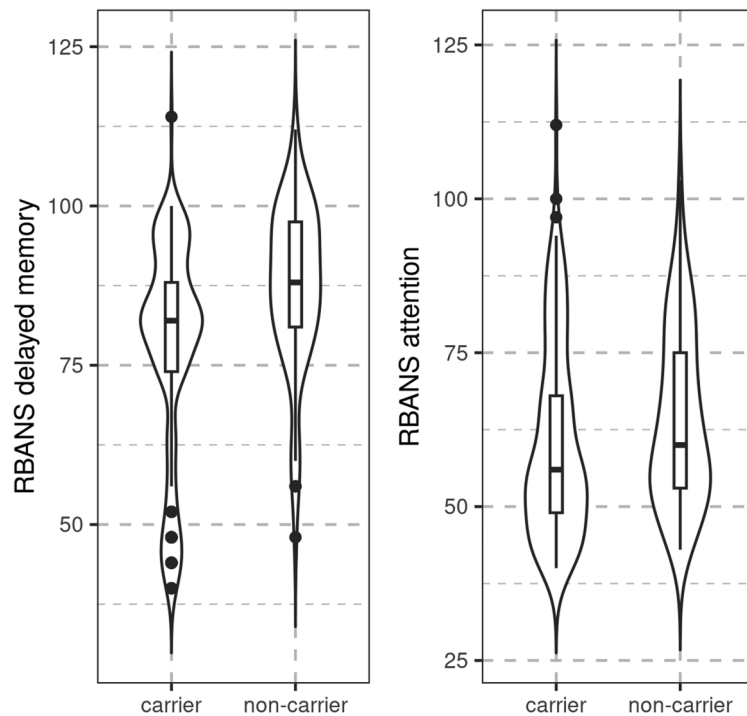
Figure 2. Association of carrier status with cognitive scores. Boxplots and violin plots featuring distribution of cognitive scores of delayed recall memory and attention according to mutation carrier status.
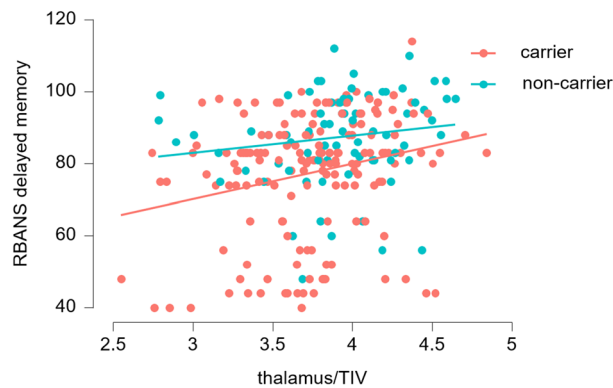

Figure 3. Association of thalamus volume with delayed recall across. Scatter plot of delayed recall regressed on thalamus volume (normalized to total intracranial volume) split according to mutation carrier status.

mutation carrier status on thalamus volume was fully mediated by the global AV45-PET signal, accounting for 87% of the covariance (Supplementary Fig. 3).

Discussion

Contrary to our primary hypothesis, we found evidence against an association of mutation carrier status with basal forebrain volume. In sporadic AD, atrophy of cholinergic basal forebrain is an early event and detectable in prodromal and even in preclinical stages of the disease[5–9]. Here, we found evidence against atrophy of the basal forebrain in preclinical and prodromal ADAD related to a PSEN1 E280A mutation. Basal forebrain atrophy has not been studied before in ADAD and also pathological studies have not investigated involvement of cholinergic basal forebrain neurons in ADAD cases. A cortical nicotinergic receptor deficit has been described in Swedish mutation carriers, however, this was based on autopsy in advanced stages of AD[31]. Preclinical studies demonstrated pathology of the cholinergic basal forebrain in transgenic mice with double or single amyloid precursor protein (APP) and presenilin1 mutations[32–35]. Specifically, in addition to confirming the presence of amyloid plaques, these studies showed a significant decrease in hippocampal choline acetyltransferase (ChAT) activity[32], metabolic changes and DNA damage in basal forebrain[35], no evidence of tau pathology but extensive inflammatory glial responses and increased trophic effects[34]. In contrast, one study analyzing ChAT activity, ChAT

	Delayed recall β [95% credible interval] + BF_{10}	Attention β [95% credible interval] + BF_{10}
CDR 0 cases		
Basal forebrain	53.9 [−14.7 to 122.5] $BF_{10} = 0.686$	−50.1 [−112.0 to 11.5] $BF_{10} = 0.508$
Hippocampus	13.6 [−2.2 to 29.4] $BF_{10} = 0.996$	−7.4 [−21.3 to 6.5] $BF_{10} = 0.246$
Thalamus	6.2 [1.6 to 10.8] $BF_{10} = 6.4$	−1.8 [−6.0 to 2.4] $BF_{10} = 0.205$
CDR 0 + 0.5 cases		
Basal forebrain	59.8 [−10.6 to 130.6] $BF_{10} = 0.851$	−47.6 [−106.2 to 11.8] $BF_{10} = 0.457$
Hippocampus	12.8 [−2.5 to 5.8] $BF_{10} = 0.797$	−5.8 [−18.7 to 7.0] $BF_{10} = 0.186$
Thalamus	6.1 [1.4 to 10.7] $BF_{10} = 6.3$	−2.5 [−6.4 to 1.4] $BF_{10} = 0.286$

Table 2. Association of brain volumes with cognitive scores. β—unstandardized parameter estimates for the association between volume and cognitive function from the ANCOVA model, controlling for age, sex, education, CDR score (in CRD 0 + 0.5 cases), and mutation carrier status.
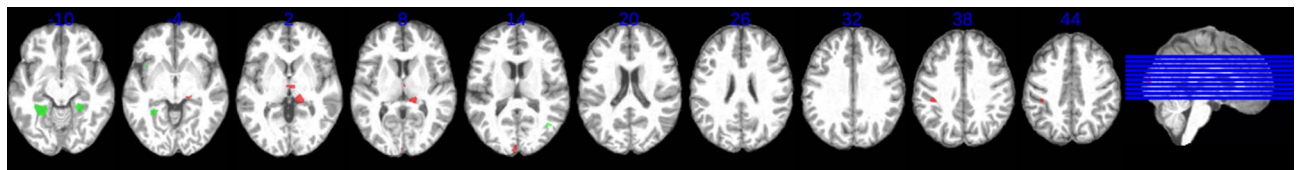

Figure 4. Association of carrier status with voxel-wide grey matter volume. Relative increase of signal in mutation carriers vs. non-carriers (green) and relative decrease in mutation carriers (red). Cluster of at least 50 voxels with p < 0.001. Blue figures on top of each scan indicate the z-coordinate in MNI space, corresponding to the level of the axial sections. Right of image is right of brain (view from superior).

mRNA level, cholinergic neuron number and receptor binding in mutant PSEN1, APP and PSEN1/APP mice showed evidence of intact basal cholinergic innervation, even in the presence of extensive amyloid pathology[36]. Our results raise the question whether these findings are transferable to humans with such mutations.

Similar to the basal forebrain, we found evidence against atrophy of the hippocampus in the PSEN1 E280A mutation carriers. This finding in the relatively large cohort agrees with previous studies on subsamples of less than 30 asymptomatic carriers and 30 noncarriers each of the Colombian kindred that revealed no statistically significant reductions in hippocampal volume[19,20,24]. Likewise, a study in ADAD mutations other than PSEN1 E280A found no hippocampus atrophy in nine asymptomatic mutation carriers compared with nine control subjects, and even when 12 MCI mutation carriers were considered, the hippocampus was spared atrophy[21]. In carriers of different APP, PSEN1, and PSEN2 mutations, hippocampal atrophy was found from approximately 5 years before[17] to 8 years after the expected onset of the disease[37], indicating a large variation of hippocampus atrophy trajectories across different mutations.

Interestingly, children and adolescents with the Colombian PSEN1 E280A mutation at age 9–17 years showed increased hippocampus, parahippocampus, and parietal and temporal lobe volumes compared with non-carriers[38]. Similarly, a study of individuals with different PSEN1 mutations found a significant increase of cortical thickness in parietotemporal regions in six asymptomatic mutation carriers on average 9.9 years before expected age of onset[39]. This is also consistent with a study in seven PSEN1 mutation carriers, distinct from the Colombian kindred, who showed accelerated hippocampus atrophy with transition to a symptomatic stage, but did not differ from controls in hippocampus volumes before this transition[18]. Similarly, in a cross-sectional analysis, cortical thickness in PSEN1 E280A carriers was higher in children and adolescent mutation carriers compared to age-matched noncarriers[40]. The underlying mechanisms of the volume increases in young asymptomatic individuals with PSEN1 mutations are currently unresolved. The PSEN1 E280A mutation may be associated with early developmental changes or neuroinflammation with glial activation or neuronal hypertrophy[41] in response to neurotoxic amyloid and lead to early apparent increase of volume in AD vulnerable regions, only later followed by neurodegeneration and related brain atrophy. This also fits with the observation from mutation carriers of the DIAN cohort that did not show differences to non-carriers in hippocampus volume at an asymptomatic baseline, but mild rates of hippocampus atrophy were followed by a strong increase of rates of volume loss only after symptom onset[42,43]. The lack of hippocampal atrophy in our analysis may therefore reflect the asymptomatic to early symptomatic stage of PSEN1 E280A mutation carriers, in which there may be a transition from a developmental increase to a neurodegenerative decrease in hippocampal volume.
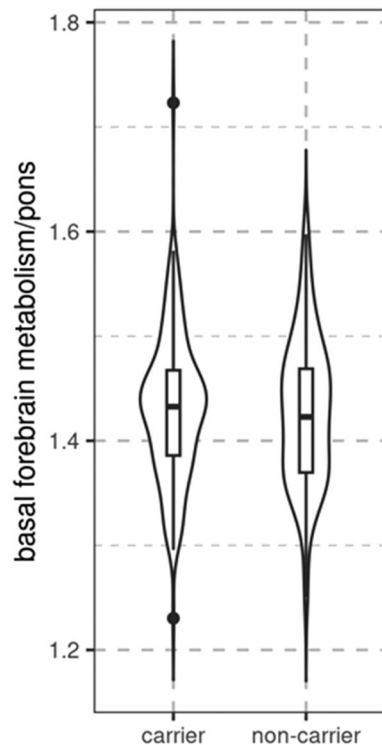
Figure 5. Association of carrier status with basal forebrain FDG-PET signal. Boxplot and violin plot featuring distribution of FDG-PET signal of the basal forebrain normalized to pons signal, according to mutation carrier status.

A possible effect similar to that seen in the hippocampus, with increased volume in young asymptomatic ADAD mutation carriers, has not yet been investigated for the basal forebrain, leaving open whether the lack of atrophy in our analysis represents a possible transitional phenomenon from developmental changes to neurodegeneration.

Several studies, mostly using voxel-based analyses, reported atrophy of the thalamus in asymptomatic mutation carriers[21–23], including individuals of the Colombian kindred[24], reviewed in[44]. Early atrophy of the thalamus in ADAD is consistent with the early deposition of amyloid in this region and the striatum as shown using amyloid sensitive PIB-PET imaging in mutation carriers from the DIAN study[22]. Here, we found that atrophy of the thalamus, but not the basal forebrain or hippocampus[20], was associated with a decrease in delayed memory performance in mutation carriers, both when considering all cases and when considering only asymptomatic cases. One study in a small sample of the Colombian kindred did not find a difference in whole thalamus volume and thalamic subregion volumes between mutation carriers and non-carriers, despite numerically larger volumes in the noncarriers[45].

Consistent with our primary hypothesis, we found evidence for a preserved metabolism of basal forebrain in mutation carriers, consistent with previous studies in sporadic prodromal AD[13,14]. Regions with relatively preserved metabolism included basal forebrain, thalamus and hippocampus in the voxel based analysis. In contrast, other PSEN1 mutations showed pronounced hypometabolism of hippocampus in asymptomatic stages[46], however, basal forebrain metabolism had not been assessed before. Hypometabolism in our analysis was mainly detected in superior parietal cortex, precuneus, and posterior cingulate gyrus, resembling the topography of cortical thickness reductions in the DIAN cohort asymptomatic mutation carriers[47] and the typical pattern of hypometabolism found in sporadic cases with amnestic or amyloid positive MCI[48].

Amyloid load was much more pronounced in the mutation carriers than the non-carriers, consistent with the presence of a PSEN1 mutation and the young age of the cohort that implied a low risk for cerebral amyloidosis in non-mutation carriers. Different to previous analyses in sporadic prodromal and preclinical AD cases[10–12], we only found anecdotal evidence for an association of global amyloid load with basal forebrain volume. In contrast, evidence was very strong for an association of global amyloid load with thalamus volume, and amyloid load fully mediated the association of mutation carrier status with thalamus volume. This is consistent with the pathogenic role of the PSEN1 E280A mutation leading to early-onset cerebral amyloidosis as the main determinant of subsequent neurodegeneration and cognitive decline[49].

Limitations

We note the following limitations of this study: we lacked longitudinal follow-up since the study participants were included in the ongoing API ADAD Colombia trial so that access to longitudinal data was not possible.
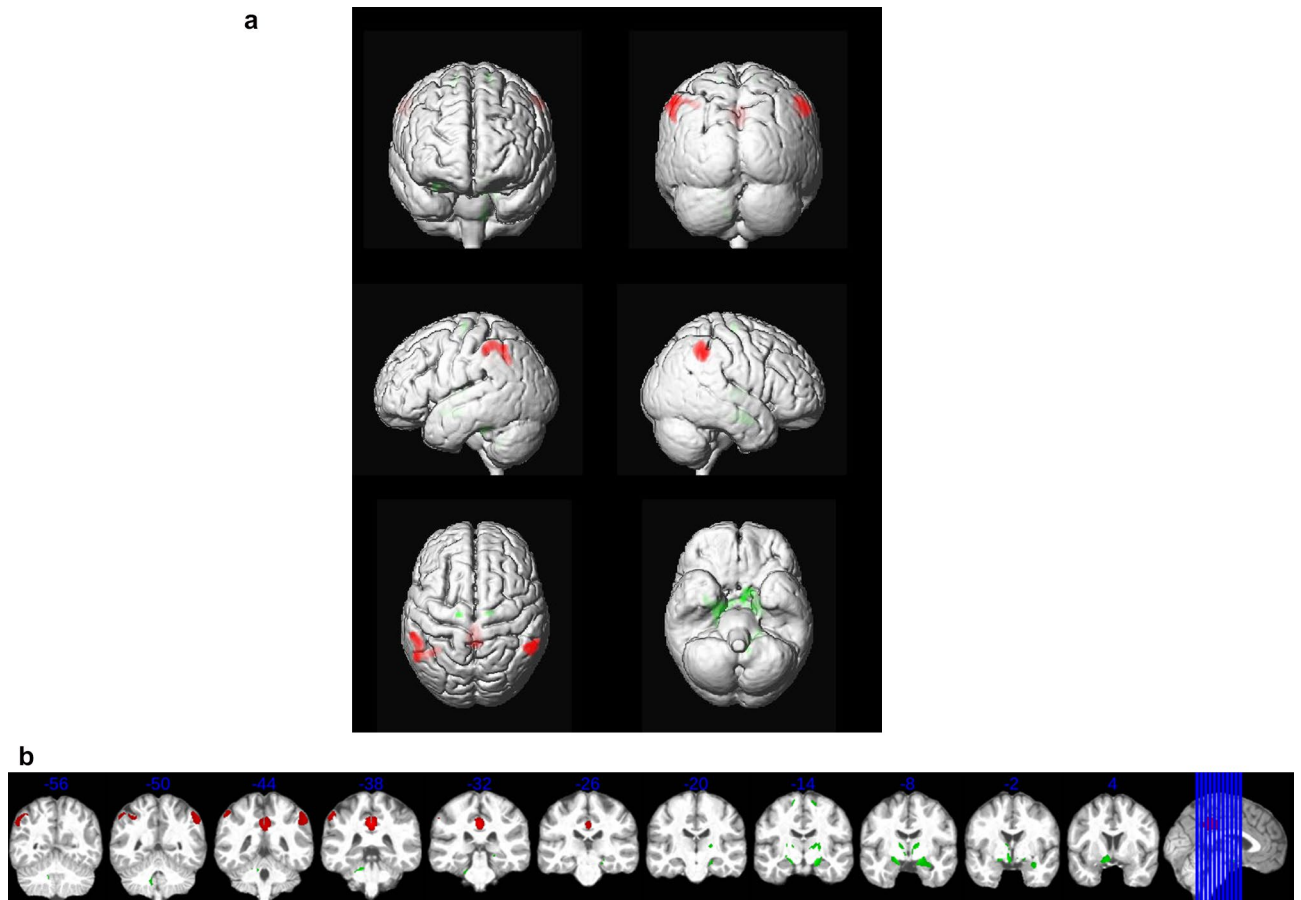
a

b

Figure 6. Voxel-wise association of carrier status with FDG-PET signal. (**a**) Effects projected on the rendered surface of an MRI scan in MNI space. Relative increase of signal in mutation carriers vs. non-carriers (green) and relative decrease in mutation carriers (red). Cluster of at least 50 voxels with p < 0.001. (**b**) Projection on coronal brain slices. Relative increase of signal in mutation carriers vs. non-carriers (green) and relative decrease in mutation carriers (red). Cluster of at least 50 voxels with p < 0.001. Blue figures on top of each coronal scan indicate the y-coordinate in MNI space, corresponding to the level of the coronal sections. Right of image is right of brain (view from posterior).

We also lacked information on the expected age of onset for the asymptomatic mutation carriers, which would have been very interesting to study in association with brain volumes and metabolism. The homogeneity of the genetic background is both an advantage and a disadvantage. It shows that the pathomechanistic effects of the PSEN1 E280A mutation lead to early involvement of thalamus but not of basal forebrain or hippocampus. It needs, however, to be shown if these results generalize to other presenilin1 mutations and even to presenilin2 and APP mutations. Basal forebrain volume and metabolism are surrogate markers for the integrity of the cholinergic basal forebrain, but not a direct estimate of neuronal structural and functional integrity[3]. However, the methods applied here match similar studies in sporadic AD allowing a direct comparison.

Conclusions

In this study, basal forebrain volume was not decreased in non-demented mutation carriers for ADAD and basal forebrain metabolism was relatively preserved. Early changes in delayed memory were associated with thalamus but not basal forebrain and hippocampus volume pointing to a different involvement of subcortical brain regions and relative sparing of cholinergic projection sites in prodromal ADAD compared with sporadic AD. This study highlights the importance of alternative disease mechanisms in ADAD and sporadic AD, at least for the PSEN1 E280A mutation, that may be relevant to understand different pathogenic roles of amyloid pathology for regional brain atrophy and metabolic changes in early stages of ADAD and sporadic AD. These findings may also have implications for considering initiation of cholinergic treatment not only in prodromal sporadic AD, but also in prodromal cases of ADAD.

Material and methods

Data source

Data were made available from the Alzheimer's Prevention Initiative (API) Autosomal-Dominant Alzheimer's Disease Colombia Trial (NCT01998841) baseline data[50]. The trial design has been described before[51]. Originally,

252 participants had been enrolled, however, data on 10 participants had to be excluded already from the trial baseline data presentation[52] to protect their confidentiality, genetic status, and trial integrity. Informed consent was obtained from all participants and study partners before any study related procedures were conducted. The trial was approved by the Colombian Health Authority (Instituto Nacional de Vigilancia de Medicamento). All consent procedures were conducted in accordance with international and local ethics committee standards and after ethics committee approval. All research was performed in accordance with relevant guidelines and regulations, including the Helsinki Declaration of 1975 and its later amendments.

Adherence to STROBE reporting guidelines is documented in Supplementary Table 2.

Participants
The API Colombia trial included individuals who carry the PSEN1 E280A autosomal-dominant mutation[15], do not meet criteria for MCI[53] or dementia due to AD[54], and are between ≥ 30 years and ≤ 60 years of age[51]. In addition, age- and sex matched members of the same kindred without the mutation were included. Detailed inclusion and exclusion criteria can be found in[51].

Cognitive measures
Measures included Clinical Dementia Rating (CDR) global score[55] which we used for stratifying participants in unimpaired (CDR = 0) and slightly impaired (CDR = 0.5) samples. In addition, we used the Repeatable Battery for the Assessment of Neuropsychological Status (RBANS) Memory and attention scores[56].

Image data acquisition
MRI data acquisition
Volumetric MR imaging data were acquired on a 1.5-T imaging system (Avanto; Siemens) with a T1-weighted, magnetization-prepared, rapid-acquisition, gradient-echo pulse sequence (echo time, minimum full; flip angle, 8°; number of excitations, 1; field of view, 22 cm; imaging matrix, 192 × 192 pixels; and section thickness, 1.2 mm).

FDG PET data acquisition
FDG-PET images were acquired on a Siemens/CTI Biograph PET/CT system, using intravenous administration of 5 mCi (185 million Bq) of FDG after a 30-min radiotracer uptake period when resting with open eyes in a darkened room, followed by a 30-min dynamic emission scan (six 5-min frames). Images were reconstructed with computed tomographic attenuation correction.

Amyloid PET data acquisition
Florbetapir scans were acquired on the same Siemens Biograph PET/CT system as the FDG-PET data, using an intravenous bolus injection of ~ 11 mCi (9.3–14.7 mCi) of florbetapir, a CT scan for correction of radiation attenuation, a 50-min radiotracer uptake-period, and a 20-min dynamic emission scan in four frames (4 × 300 s)[57]. PET images were reconstructed using an ordered subset expectation maximization (OSEM) algorithm and attenuation-corrected, frames were evaluated for adequate count statistics and absence of head motion[57].

Image data processing
MRI data
MRI data were processed by using statistical parametric mapping (SPM12, Wellcome Trust Center for Neuroimaging) and the CAT12.3-toolbox (http://dbm.neuro.uni-jena.de/cat) implemented in MATLAB R2019 (MathWorks, Natick, MA). First, MRI scans were automatically segmented into grey matter (GM), white matter (WM) and cerebrospinal fluid (CSF) partitions of 1.5 mm isotropic voxel-size using the prior free Adaptive Maximum A Posterior (AMAP) segmentation routine of the CAT12-toolbox. The resulting GM and WM partitions of each subject in native space were then high-dimensionally registered to the MNI reference template using the DARTEL algorithm[58]. Individual flow-fields resulting from the DARTEL registration to the reference template were used to warp the GM segments and voxel-values were modulated for volumetric changes introduced by the high-dimensional normalization, such that the total amount of GM volume present before warping was preserved. For extraction of basal forebrain volume, we used a cytoarchitectonic map of BF cholinergic nuclei in MNI space, derived from combined histology and MRI of a post-mortem brain, as described previously[59]. Hippocampus and thalamus volumes were derived using the Hammers brain atlas regions of interest[60].

PET data
Images were preprocessed using SPM12 implemented in Matlab 2019[61]. First, each subject's averaged PET frames were co-registered to their corresponding T1-weighted MRI scan. Then, the coregistered PET images were spatially normalized to the MNI reference template using the deformation parameters derived from the normalization of their corresponding MRI scans.

For extraction of Florbetapir SUVR we used the Centiloid cortical mask and normalized the PET signal to the whole cerebellum Centiloid mask[62]. For FDG-PET we extracted regional SUVR values using the basal forebrain region and Hammers brain atlas regions of interest for hippocampus and thalamus[60], and normalized the PET signal to the signal of the pons.

Statistical analysis
For region of interest based analyses we used Bayesian ANCOVA with *Bayes factor (BF) hypothesis testing* with volume or metabolism as dependent variable, mutation carrier status as independent variable, and age, sex, CDR

score, and (for analyses of cognitive scores) education as confounders, to compare the alternative hypothesis against the null hypothesis (i.e., the assumption that there is an effect of carrier status, H_1)[26,27], as implemented in *Jeffreys' Amazing Statistics Program* (JASP Version 0.16.4), available at jasp-stats.org.

We report the Bayes Factor (BF_{10}) quantifying evidence in favor of the alternative hypotheses. Three conclusions are possible within the Bayesian framework[26]: support for either the null hypothesis ($BF_{10} \leq 0.33$), support for the alternative hypothesis ($BF_{10} > 3$), or inconclusive evidence (BF_{10} between 0.33 and 3). We applied the following evidence categories: a BF_{10} above 3 provides "substantial evidence", a BF_{10} above 10 provides "strong evidence", a BF_{10} above 30 provides "very strong evidence" and a BF_{10} above 100 provides "extreme evidence" against the null model[63].

For data driven analysis we conducted voxel based analysis of grey matter maps and normalized FDG-PET data scaled to pons signal, respectively, using spm12, implemented in Matlab version 2020a. We regressed voxelwise grey matter or FDG signal on carrier status, controlled for age, sex, and CDR score. We considered clusters of at least 50 voxel passing an uncorrected p-value of 0.001.

Data availability

Data are available from the authors upon reasonable request and with the permission of the Banner Alzheimer's Foundation. The Alzheimer's Prevention Initiative website hosts materials and details regarding the API ADAD Trial and data sharing process for review or download at https://alzheimerspreventioninitiative.com.

References

1. Auld, D. S., Kornecook, T. J., Bastianetto, S. & Quirion, R. Alzheimer's disease and the basal forebrain cholinergic system: Relations to beta-amyloid peptides, cognition, and treatment strategies. *Prog. Neurobiol.* **68**, 209–245 (2002).
2. Schliebs, R. & Arendt, T. The cholinergic system in aging and neuronal degeneration. *Behav. Brain Res.* **221**, 555–563. https://doi.org/10.1016/j.bbr.2010.11.058 (2011).
3. Teipel, S. J., Fritz, H. C., Grothe, M. J., Alzheimer's Disease Neuroimaging Initiative. Neuropathologic features associated with basal forebrain atrophy in Alzheimer disease. *Neurology* **95**, e1301–e1311. https://doi.org/10.1212/WNL.0000000000010192 (2020).
4. Mufson, E. J. *et al.* Mild cognitive impairment: Pathology and mechanisms. *Acta Neuropathol.* **123**, 13–30. https://doi.org/10.1007/s00401-011-0884-1 (2012).
5. Grothe, M. *et al.* Reduction of basal forebrain cholinergic system parallels cognitive impairment in patients at high risk of developing Alzheimer's disease. *Cereb. Cortex* **20**, 1685–1695. https://doi.org/10.1093/cercor/bhp232 (2010).
6. Grothe, M. J. *et al.* Cognitive correlates of basal forebrain atrophy and associated cortical hypometabolism in mild cognitive impairment. *Cereb. Cortex* https://doi.org/10.1093/cercor/bhv062 (2015).
7. Muth, K. *et al.* Mild cognitive impairment in the elderly is associated with volume loss of the cholinergic basal forebrain region. *Biol. Psychiatry* **67**, 588–591. https://doi.org/10.1016/j.biopsych.2009.02.026 (2010).
8. Herdick, M. *et al.* Multimodal MRI analysis of basal forebrain structure and function across the Alzheimer's disease spectrum. *Neuroimage Clin.* **28**, 102495. https://doi.org/10.1016/j.nicl.2020.102495 (2020).
9. Richter, N. *et al.* Age and anterior basal forebrain volume predict the cholinergic deficit in patients with mild cognitive impairment due to Alzheimer's disease. *J. Alzheimers Dis.* **86**, 425–440. https://doi.org/10.3233/JAD-210261 (2022).
10. Grothe, M. J. *et al.* Basal forebrain atrophy and cortical amyloid deposition in nondemented elderly subjects. *Alzheimers Dement.* **10**, S344–S353. https://doi.org/10.1016/j.jalz.2013.09.011 (2014).
11. Kerbler, G. M. *et al.* Basal forebrain atrophy correlates with amyloid beta burden in Alzheimer's disease. *Neuroimage Clin.* **7**, 105–113. https://doi.org/10.1016/j.nicl.2014.11.015 (2015).
12. Teipel, S. *et al.* Cholinergic basal forebrain atrophy predicts amyloid burden in Alzheimer's disease. *Neurobiol. Aging* **35**, 482–491. https://doi.org/10.1016/j.neurobiolaging.2013.09.029 (2014).
13. Kim, M. J. *et al.* Increased basal forebrain metabolism in mild cognitive impairment: An evidence for brain reserve in incipient dementia. *J. Alzheimers Dis.* **32**, 927–938. https://doi.org/10.3233/JAD-2012-120133 (2012).
14. Nicolas, B. *et al.* Basal forebrain metabolism in Alzheimer's disease continuum: Relationship with education. *Neurobiol. Aging* **87**, 70–77. https://doi.org/10.1016/j.neurobiolaging.2019.11.013 (2020).
15. Lendon, C. L. *et al.* E280A PS-1 mutation causes Alzheimer's disease but age of onset is not modified by ApoE alleles. *Hum. Mutat.* **10**, 186–195. https://doi.org/10.1002/(SICI)1098-1004(1997)10:3%3c186::AID-HUMU2%3e3.0.CO;2-H (1997).
16. Lopera, F. *et al.* Clinical features of early-onset Alzheimer disease in a large kindred with an E280A presenilin-1 mutation. *JAMA* **277**, 793–799 (1997).
17. Ridha, B. H. *et al.* Tracking atrophy progression in familial Alzheimer's disease: A serial MRI study. *Lancet Neurol.* **5**, 828–834. https://doi.org/10.1016/S1474-4422(06)70550-6 (2006).
18. Fox, N. C. *et al.* Presymptomatic hippocampal atrophy in Alzheimer's disease. A longitudinal MRI study. *Brain* **119**(Pt 6), 2001–2007. https://doi.org/10.1093/brain/119.6.2001 (1996).
19. Norton, D. J. *et al.* Subjective memory complaints in preclinical autosomal dominant Alzheimer disease. *Neurology* **89**, 1464–1470. https://doi.org/10.1212/WNL.0000000000004533 (2017).
20. Vila-Castelar, C. *et al.* Examining sex differences in markers of cognition and neurodegeneration in autosomal dominant Alzheimer's disease: Preliminary findings from the Colombian Alzheimer's prevention initiative biomarker study. *J. Alzheimers Dis.* **77**, 1743–1753. https://doi.org/10.3233/JAD-200723 (2020).
21. Lee, G. J. *et al.* Regional brain volume differences in symptomatic and presymptomatic carriers of familial Alzheimer's disease mutations. *J. Neurol. Neurosurg. Psychiatry* **84**, 154–162. https://doi.org/10.1136/jnnp-2011-302087 (2013).
22. Benzinger, T. L. *et al.* Regional variability of imaging biomarkers in autosomal dominant Alzheimer's disease. *Proc. Natl. Acad. Sci. USA* **110**, E4502–E4509. https://doi.org/10.1073/pnas.1317918110 (2013).
23. Ryan, N. S. *et al.* Magnetic resonance imaging evidence for presymptomatic change in thalamus and caudate in familial Alzheimer's disease. *Brain* **136**, 1399–1414. https://doi.org/10.1093/brain/awt065 (2013).
24. Fleisher, A. S. *et al.* Associations between biomarkers and age in the presenilin 1 E280A autosomal dominant Alzheimer disease kindred: A cross-sectional study. *JAMA Neurol.* **72**, 316–324. https://doi.org/10.1001/jamaneurol.2014.3314 (2015).
25. Temp, A. G. M. *et al.* How Bayesian statistics may help answer some of the controversial questions in clinical research on Alzheimer's disease. *Alzheimers Dement.* **17**, 917–919. https://doi.org/10.1002/alz.12374 (2021).
26. Wagenmakers, E. J. *et al.* Bayesian inference for psychology. Part I: Theoretical advantages and practical ramifications. *Psychon. B Rev.* **25**, 35–57. https://doi.org/10.3758/s13423-017-1343-3 (2018).

27. Goodman, S. A dirty dozen: Twelve P-value misconceptions. *Semin. Hematol.* **45**, 135–140. https://doi.org/10.1053/j.seminhematol.2008.04.003 (2008).
28. Kruschke, J. K. *Doing Bayesian Data Analysis—A Tutorial with R, JAGS, and Stan*, 2nd edn, 87–89, 317–325 (Elsevier, 2015).
29. Naimi, A. I. & Whitcomb, B. W. Can confidence intervals be interpreted?. *Am. J. Epidemiol.* **189**, 631–633. https://doi.org/10.1093/aje/kwaa004 (2020).
30. Mullane, K. & Williams, M. Preclinical models of Alzheimer's disease: Relevance and translational validity. *Curr. Protoc. Pharmacol.* **84**, e57. https://doi.org/10.1002/cpph.57 (2019).
31. Marutle, A., Warpman, U., Bogdanovic, N., Lannfelt, L. & Nordberg, A. Neuronal nicotinic receptor deficits in Alzheimer patients with the Swedish amyloid precursor protein 670/671 mutation. *J. Neurochem.* **72**, 1161–1169. https://doi.org/10.1046/j.1471-4159.2000.0721161.x (1999).
32. Laursen, B., Mork, A., Plath, N., Kristiansen, U. & Bastlund, J. F. Cholinergic degeneration is associated with increased plaque deposition and cognitive impairment in APPswe/PS1dE9 mice. *Behav. Brain Res.* **240**, 146–152. https://doi.org/10.1016/j.bbr.2012.11.012 (2013).
33. Wang, Y., Greig, N. H., Yu, Q. S. & Mattson, M. P. Presenilin-1 mutation impairs cholinergic modulation of synaptic plasticity and suppresses NMDA currents in hippocampus slices. *Neurobiol. Aging* **30**, 1061–1068. https://doi.org/10.1016/j.neurobiolaging.2007.10.009 (2009).
34. Jaffar, S. *et al.* Neuropathology of mice carrying mutant APP(swe) and/or PS1(M146L) transgenes: Alterations in the p75(NTR) cholinergic basal forebrain septohippocampal pathway. *Exp. Neurol.* **170**, 227–243. https://doi.org/10.1006/exnr.2001.7710 (2001).
35. Strazielle, C., Rozat, J., Verdier, Y., Qian, S. & Lalonde, R. Regional brain metabolism with cytochrome c oxidase histochemistry in a PS1/A246E mouse model of autosomal dominant Alzheimer's disease: Correlations with behavior and oxidative stress. *Neurochem. Int.* **55**, 806–814 (2009).
36. Hernandez, D. *et al.* Survival and plasticity of basal forebrain cholinergic systems in mice transgenic for presenilin-1 and amyloid precursor protein mutant genes. *Neuroreport* **12**, 1377–1384 (2001).
37. Yau, W. W. *et al.* Longitudinal assessment of neuroimaging and clinical markers in autosomal dominant Alzheimer's disease: A prospective cohort study. *Lancet Neurol.* **14**, 804–813. https://doi.org/10.1016/S1474-4422(15)00135-0 (2015).
38. Quiroz, Y. T. *et al.* Brain imaging and blood biomarker abnormalities in children with autosomal dominant Alzheimer disease: A cross-sectional study. *JAMA Neurol.* **72**, 912–919. https://doi.org/10.1001/jamaneurol.2015.1099 (2015).
39. Fortea, J. *et al.* Increased cortical thickness and caudate volume precede atrophy in PSEN1 mutation carriers. *J. Alzheimers Dis.* **22**, 909–922. https://doi.org/10.3233/JAD-2010-100678 (2010).
40. Fox-Fuller, J. T. *et al.* Cortical thickness across the lifespan in a Colombian cohort with autosomal-dominant Alzheimer's disease: A cross-sectional study. *Alzheimers Dement (Amst)* **13**, e12233. https://doi.org/10.1002/dad2.12233 (2021).
41. Iacono, D. *et al.* Neuronal hypertrophy in asymptomatic Alzheimer disease. *J. Neuropathol. Exp. Neurol.* **67**, 578–589. https://doi.org/10.1097/NEN.0b013e3181772794 (2008).
42. Morris, J. C. *et al.* Autosomal dominant and sporadic late onset Alzheimer's disease share a common in vivo pathophysiology. *Brain* **145**, 3594–3607. https://doi.org/10.1093/brain/awac181 (2022).
43. Xiong, C. *et al.* Cross-sectional and longitudinal comparisons of biomarkers and cognition among asymptomatic middle-aged individuals with a parental history of either autosomal dominant or late-onset Alzheimer's disease. *Alzheimers Dement.* https://doi.org/10.1002/alz.12912 (2023).
44. Tentolouris-Piperas, V., Ryan, N. S., Thomas, D. L. & Kinnunen, K. M. Brain imaging evidence of early involvement of subcortical regions in familial and sporadic Alzheimer's disease. *Brain Res.* **1655**, 23–32. https://doi.org/10.1016/j.brainres.2016.11.011 (2017).
45. Pardilla-Delgado, E. *et al.* Associations between subregional thalamic volume and brain pathology in autosomal dominant Alzheimer's disease. *Brain Commun.* **3**, fcab101. https://doi.org/10.1093/braincomms/fcab101 (2021).
46. Mosconi, L. *et al.* Hypometabolism exceeds atrophy in presymptomatic early-onset familial Alzheimer's disease. *J. Nucl. Med.* **47**, 1778–1786 (2006).
47. Dincer, A. *et al.* Comparing cortical signatures of atrophy between late-onset and autosomal dominant Alzheimer disease. *Neuroimage Clin.* **28**, 102491. https://doi.org/10.1016/j.nicl.2020.102491 (2020).
48. Cohen, A. D. & Klunk, W. E. Early detection of Alzheimer's disease using PiB and FDG PET. *Neurobiol. Dis.* https://doi.org/10.1016/j.nbd.2014.05.001 (2014).
49. Dinkel, F. *et al.* Decreased deposition of beta-amyloid 1–38 and increased deposition of beta-amyloid 1–42 in brain tissue of presenilin-1 E280A familial Alzheimer's disease patients. *Front. Aging Neurosci.* **12**, 220. https://doi.org/10.3389/fnagi.2020.00220 (2020).
50. Reiman, E. M. *et al.* A public resource of baseline data from the Alzheimer's Prevention Initiative Autosomal-Dominant Alzheimer's Disease Trial. *Alzheimers Dement.* https://doi.org/10.1002/alz.12843 (2022).
51. Tariot, P. N. *et al.* The Alzheimer's Prevention Initiative Autosomal-Dominant Alzheimer's Disease Trial: A study of crenezumab versus placebo in preclinical PSEN1 E280A mutation carriers to evaluate efficacy and safety in the treatment of autosomal-dominant Alzheimer's disease, including a placebo-treated noncarrier cohort. *Alzheimers Dement. (N Y)* **4**, 150–160. https://doi.org/10.1016/j.trci.2018.02.002 (2018).
52. Rios-Romenets, S. *et al.* Baseline demographic, clinical, and cognitive characteristics of the Alzheimer's Prevention Initiative (API) Autosomal-Dominant Alzheimer's Disease Colombia Trial. *Alzheimers Dement.* **16**, 1023–1030. https://doi.org/10.1002/alz.12109 (2020).
53. Albert, M. S. *et al.* The diagnosis of mild cognitive impairment due to Alzheimer's disease: Recommendations from the National Institute on Aging-Alzheimer's Association workgroups on diagnostic guidelines for Alzheimer's disease. *Alzheimers Dement.* **7**, 270–279. https://doi.org/10.1016/j.jalz.2011.03.008 (2011).
54. McKhann, G. M. *et al.* The diagnosis of dementia due to Alzheimer's disease: Recommendations from the National Institute on Aging-Alzheimer's Association workgroups on diagnostic guidelines for Alzheimer's disease. *Alzheimers Dement.* **7**, 263–269. https://doi.org/10.1016/j.jalz.2011.03.005 (2011).
55. Morris, J. C. The Clinical Dementia Rating (CDR): Current version and scoring rules. *Neurology* **43**, 2412–2414. https://doi.org/10.1212/wnl.43.11.2412-a (1993).
56. Randolph, C., Tierney, M. C., Mohr, E. & Chase, T. N. The Repeatable Battery for the Assessment of Neuropsychological Status (RBANS): Preliminary clinical validity. *J. Clin. Exp. Neuropsychol.* **20**, 310–319. https://doi.org/10.1076/jcen.20.3.310.823 (1998).
57. Fleisher, A. S. *et al.* Florbetapir PET analysis of amyloid-beta deposition in the presenilin 1 E280A autosomal dominant Alzheimer's disease kindred: A cross-sectional study. *Lancet Neurol.* **11**, 1057–1065. https://doi.org/10.1016/S1474-4422(12)70227-2 (2012).
58. Ashburner, J. A fast diffeomorphic image registration algorithm. *Neuroimage* **38**, 95–113 (2007).
59. Kilimann, I. *et al.* Subregional basal forebrain atrophy in Alzheimer's disease: A multicenter study. *J. Alzheimers Dis.* **40**, 687–700. https://doi.org/10.3233/JAD-132345 (2014).
60. Hammers, A. *et al.* Three-dimensional maximum probability atlas of the human brain, with particular reference to the temporal lobe. *Hum. Brain Mapp.* **19**, 224–247 (2003).
61. Grothe, M. J. *et al.* In vivo staging of regional amyloid deposition. *Neurology* **89**, 2031–2038. https://doi.org/10.1212/WNL.0000000000004643 (2017).
62. Klunk, W. E. *et al.* The Centiloid Project: Standardizing quantitative amyloid plaque estimation by PET. *Alzheimers Dement.* **11**(1–15), e11–e14. https://doi.org/10.1016/j.jalz.2014.07.003 (2015).

63. Wagenmakers, E. J. *et al.* Bayesian inference for psychology. Part II: Example applications with JASP. *Psychon. B Rev.* **25**, 58–76. https://doi.org/10.3758/s13423-017-1323-7 (2018).

Author contributions
S.T contributed writing of the manuscript, analyzing the data, and planning the study. A.G. contributed revising the manuscript and supporting the analysis. M.D. contributed revising the manuscript and supporting the analysis. M.J.G. contributed revising the manuscript and supporting the analysis. N.P. contributed revising the manuscript and supporting the analysis and the planning of the study.

Competing interests
S.T. served as member of advisory boards of Lilly, Eisai, and Biogen, and is member of the independent data safety and monitoring board of the study ENVISION (Biogen). A.G., M.D., M.J.G., and N.P. report no competing interests.

Additional information
Supplementary Information The online version contains supplementary material available at https://doi.org/10.1038/s41598-024-60799-9.

Correspondence and requests for materials should be addressed to S.T.

Reprints and permissions information is available at www.nature.com/reprints.

Publisher's note Springer Nature remains neutral with regard to jurisdictional claims in published maps and institutional affiliations.